Solid State Communications 251 (2017) 50–59

Contents lists available at ScienceDirect

Solid State Communications

journal homepage: www.elsevier.com/locate/ssc

Communication

Half-metallicity and magnetism of the full-Heusler compounds KYX_2 (Y=Ti, V, and Cr; X=C, N, and O)

M. Dehghanzadeh, F. Ahmadian*

Department of Physics, Shahreza Branch, Islamic Azad University, Shahreza, Iran

ARTICLE INFO

Keywords:
A. Half-metals
A. Heusler alloys
D. Magnetic properties
D. Electronic properties

ABSTRACT

The electronic structure and half-metallic (HM) properties of new alloys KYX_2 (Y=Ti, V, and Cr; X=C, N, and O) containing transition metals and *sp* elements were investigated within the density functional theory (DFT) using the self-consistent full-potential linearized augmented plane wave (FPLAPW) method. It was found that these new compounds can be experimentally synthesized because of their negative formation energies. The total energy calculations showed that in all compounds, the stable state structure was a ferromagnetic $AlCu_2Mn$-type structure except for $KTiC_2$ and $KTiN_2$ which were stable in a nonmagnetic (NM) $AlCu_2Mn$-type structure. The $KTiO_2$ in both structures, $KCrO_2$ in $AlCu_2Mn$-type structure, and KVO_2 in $CuHg_2Ti$-type structure were half-metallic ferromagnets. KVO_2 in $AlCu_2Mn$-type structure was a special case with a ferromagnetic semiconducting behavior. The origin of minority band gaps for $KTiO_2$ in both structures was also studied using the band structure calculations. The total magnetic moments of HM compounds were integer values which were in agreement with Slater-Pauling rule ($M_{tot}=Z_{tot}-12$). Furthermore, the regions of half-metallictiy in HM compounds were considerably wider than those of Heusler compounds including transition metals, indicating the high robustness of half-metallicity with variation of lattice constants.

1. Introduction

Half-Metallic (HM) ferromagnets are interesting materials that acts as conductors to one channel spin and as insulator or semiconductor to another spin channel [1,2]. These substances are promising magnetic materials for spintronic applications (i.e., spin dependent electronics). De Groot et al. [1] firstly predicted HM characteristic in the NiMnSb half-Heusler alloy in 1983. Until now, various HM ferromagnets have been discovered and investigated, such as full-Heusler alloys such as Co_2MnSi [3] and Co_2CrAl [4], rutile-type CrO_2 [5], spinel Fe_3O_4 [6], pyrite structure CoS_2 [7], double perovskite Sr_2FeMoO_6 [8], perovskite $La_{0.7}Sr_{0.3}MnO_3$ [9], and some diluted magnetic semiconductors [10–13].

Due to structural similarity to the semiconductors with zinc blende (ZB) structure and the relatively high Curie temperature in Heusler alloys, they are attractive and have important role in the field of efficient spin injection from a ferromagnet to a semiconductor [14–18]. HM Heusler alloys mainly contain transition metals such as Co_2MSi (M=Ti, V, and Cr) [19], Co_2MnZ where Z is a *sp* element [20], Co_2TiZ (Z=Si, Ge, and Sn) [21], Mn_2CoZ (Z = Al, Ga, Si, Ge, Sn, and Sb) [22], Fe_2MnP [23], Fe_2TiP [24], Cr_2MnZ (Z = P, As, Sb, Bi, and Al) [25,26], V_2YSb (Y=Cr, Mn, Fe, and Co) [27], and Ti_2YZ (Y = Fe, Co, Ni; Z = Al, Ga, In) [28].

Recently, new classes of half-metals without transition metals, such as, the graphene nanoribbon [29], the alkaline-earth carbides, and nitrides with zinc-blende and rocksalt structures [30–35] have been investigated. These materials are usually called *sp* or d^0 half-metals and mainly have small magnetic moments, low stray fields, and energy loss which make them more preferable in spintronic device applications. There are a few studies on Heusler alloys without transition metals. Rozale et al. [36] investigated HM characteristic of full-Heusler $KCaX_2$ (X=C, N, and O) compounds and found that both $KCaN_2$ and $KCaO_2$ compounds were HM ferromagnets. Afterwards, $RbSrX_2$ (X=C, N, and O) compounds were investigated [37]. $RbSrC_2$ in the $AlCu_2Mn$- and $CuHg_2Ti$-type structures was a nonmagnetic metal and $RbSrN_2$ and $RbSrO_2$ compounds in both structures were HM ferromagnets. Furthermore, calculations on $CsBaX_2$ (X=C, N, and O) Heusler compounds showed that $CsBaC_2$ in the $AlCu_2Mn$-type and $CsBaN_2$ and $CsBaO_2$ compounds in both structures were half-metallic ferromagnets, while $CsBaC_2$ in $CuHg_2Ti$-type structure was a nonmagnetic metal [38]. Nowadays, great theoretical efforts are done to find new members of HM ferromagnets since synthesis of stoichiometric compositions are very complex. In this paper, Heusler alloys KYX_2 (Y=Ti, V, and Cr; X=C, N, and O) which are the combination of transition

* Corresponding author.
E-mail addresses: farzad.ahmadian@gmail.com, ahmadian@iaush.ac.ir (F. Ahmadian).

http://dx.doi.org/10.1016/j.ssc.2016.12.014
Received 6 November 2016; Accepted 20 December 2016
Available online 21 December 2016

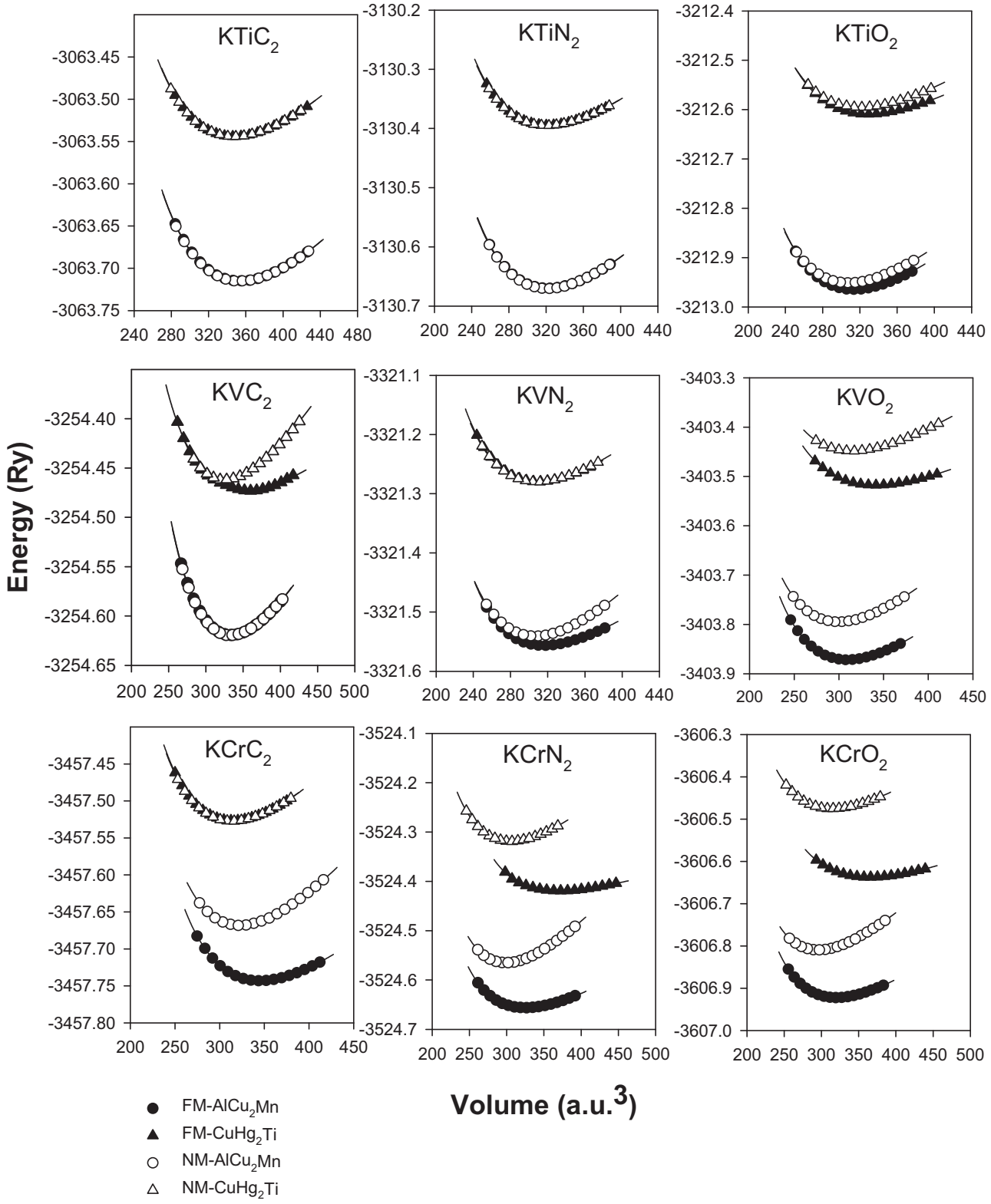

Fig. 1. Total energy as a function of unit cell volume for the KYX_2 (Y=Ti, V, and Cr; X=C, N, and O) alloys for $AlCu_2Mn$ and $CuHg_2Ti$-type structures in the ferromagnetic (FM) and non-magnetic (NM) states.

metals and *sp* elements are studied. To the best our knowledge, there is no experimental or theoretical report on the half-metallicity of these combined alloys. The electronic structure and magnetism of KYX_2 (Y=Ti, V, and Cr; X=C, N, and O) compounds for both $AlCu_2Mn$ and $CuHg_2Ti$-type structures were calculated and investigated.

2. Computational method

The WIEN2K code [39] was used to study the electronic and magnetic properties of KYX_2 (Y=Ti, V, and Cr; X=C, N, and O) compounds within density functional theory (DFT) using full potential linearized augmented plane wave (FPLAPW) method. In this method,

Table 1
The calculated bulk parameters KYX_2(Y=Ti, V, and Cr; X=C, N, and O) compounds in $AlCu_2Mn$-type and $CuHg_2Ti$-type structures. a(Å): lattice parameter, B(GPa):bulk module, $B^{'}$: derivative of bulk module, E_c(Ry): Cohesive energy, and E_f (Ry): Formation energy.

Compound	*Structure*	a (Å)	B (Gpa)	$B^{'}$	E_C (Ry)	E_f (Ry)
$KTiC_2$	$AlCu_2Mn$	5.95	94.98	4.18	−1.04	0.06
	$CuHg_2Ti$	5.92	84.22	4.32	−0.87	0.11
$KTiN_2$	$AlCu_2Mn$	5.77	118.86	4.34	−0.98	−0.50
	$CuHg_2Ti$	5.76	99.72	4.53	−0.71	−0.23
$KTiO_2$	$AlCu_2Mn$	5.71	118.99	4.44	−1.25	−0.73
	$CuHg_2Ti$	5.81	83.94	4.78	−0.89	−0.38
KVC_2	$AlCu_2Mn$	5.84	104.21	4.24	−0.94	0.05
	$CuHg_2Ti$	5.95	46.687	4.66	−0.80	0.20
KVN_2	$AlCu_2Mn$	5.73	94.86	5.45	−0.86	−0.37
	$CuHg_2Ti$	5.70	98.15	4.83	−0.58	−0.10
KVO_2	$AlCu_2Mn$	5.69	116.32	4.56	−1.15	−0.62
	$CuHg_2Ti$	5.88	−67.55	4.81	−0.79	−0.27
$KCrC_2$	$AlCu_2Mn$	5.90	78.91	4.65	−0.83	0.05
	$CuHg_2Ti$	5.72	92.68	4.39	−0.62	0.27
$KCrN_2$	$AlCu_2Mn$	5.78	74.49	5.19	−0.73	−0.34
	$CuHg_2Ti$	6.04	42.69	6.74	−0.49	−0.11
$KCrO_2$	$AlCu_2Mn$	5.75	96.11	4.85	−0.97	−0.54
	$CuHg_2Ti$	6.01	53.37	4.71	−0.68	−0.26

the space of unit cell is divided into muffin-tin (*MT*) spheres which are separated by an interstitial region. The wave functions are expanded in terms of spherical harmonic functions inside muffin-tin spheres and expanded terms of Fourier series in the interstitial region. The generalized-gradient approximation (GGA) [40] was employed to calculate the exchange and correlation between electrons. The muffin-tin sphere radii for all atoms were chosen 2 *a.u.*. The cut off parameter $R_{mt}K_{max}$ is equal to 8.00 where K_{max} is the largest reciprocal lattice vector used in the plane wave expansion and R_{mt} represents the smallest of the MT sphere radii. The highest orbital momentum for the wave function expansion inside atomic spheres (l_{max}) is equal to 10. For Brillouin zone (BZ) integration, a 12×12×12 mesh containing 84 irreducible k points is used. The integrated charge difference between two successive iterations for charge convergence is less than $10^{-4}e/a.u.^3$.

3. Results and discussion

3.1. Structural properties

Heusler alloys are categorized into two distinct groups by their crystalline structures; half Heusler alloys with the form of XYZ in the $C1_b$ structure and full Heusler alloys with the form of X_2YZ in the $L2_1$ structure. The unit cell of $L2_1$ structure consists of four face-centered cubic (fcc) sublattices, while that of the $C1_b$ structure is formed by removing one of the X sites. In Full-Heusler compounds in $L2_1$ structure (with a space group of $Fm\bar{3}m$), X, Y, and Z atoms are placed on the Wyckoff positions 8c (1/4, 1/4, 1/4), 4a (0, 0, 0), and 4b (1/2, 1/2, 1/2), respectively. This structure is also known as $AlCu_2Mn$-type structure. Full Heusler alloys crystallize in the other structure ($CuHg_2Ti$-type structure) with the space group of $F4\bar{3}m$ in which X atoms occupy 4a (0, 0, 0) and 4c (1/4, 1/4, 1/4) positions and Y and Z atoms are located on 4b (1/2, 1/2, 1/2) and 4d (3/4, 3/4, 3/4) positions, respectively. In this structure, the X atoms occupying sites 4a and 4c are denoted as X (1) and X (2), respectively.

In order to study the equilibrium structural properties of KYX_2 (Y=Ti, V, and Cr; X=C, N, and O) alloys, the total energy as a function of the unit cell volume per formula unit for $AlCu_2Mn$ and $CuHg_2Ti$-type structures in the ferromagnetic (FM) and non-magnetic (NM) states was calculated and fitted to the empirical Murnaghan equation of state [41]. The Energy-Volume curves for all compounds were plotted in Fig. 1. It is clear that $KCrX_2$ (X=C, N, and O), KVX_2 (X=C, N, and O), and $KTiO_2$ compounds are energetically stable in $AlCu_2Mn$-type structure in FM state, while the ground state structure of $KTiC_2$ and $KTiN_2$ compounds is $AlCu_2Mn$-type in NM state. The equilibrium parameters including the lattice parameter (a), bulk modulus (B), derivative of bulk modulus ($B^{'}$), cohesive energy (E_C), and formation energy (E_f) were presented in Table 1. There is no experimental or theoretical data to compare the obtained results with.

The relatively high values of E_C (the energy required for separating the condensed material into isolated free atoms) indicate that each alloy may be stable due to the high energy of chemical bonds.

The formation energy, which is the difference between the ground state total energy of alloys and the summation of total energies of atoms in pure bulk form, is a criterion for evaluating the synthesis of compounds, experimentally. According to Table 1, all E_f values are negative except for $KCrC_2$, $KTiC_2$, and KVC_2 in both structures which show that the three compounds cannot be synthesized experimentally and non-equilibrium growth methods should be used for synthesizing of them.

3.2. Electronic properties

In order to investigate the electronic structure of KYX_2 (Y=Ti, V, and Cr; X=C, N, and O) compounds, the spin-polarized band structures of these compounds in $AlCu_2Mn$ and $CuHg_2Ti$-type structures for majority (spin-down) and minority (spin-up) spin states were calculated. The band structures of KYO_2 (Y=Ti, V, and Cr) compounds as representative of all compounds for both structures were shown in Figs. 2–4. Accordingly, for $KTiO_2$ in both structures, the majority spin states cross the Fermi level and in the minority spin state, the Fermi

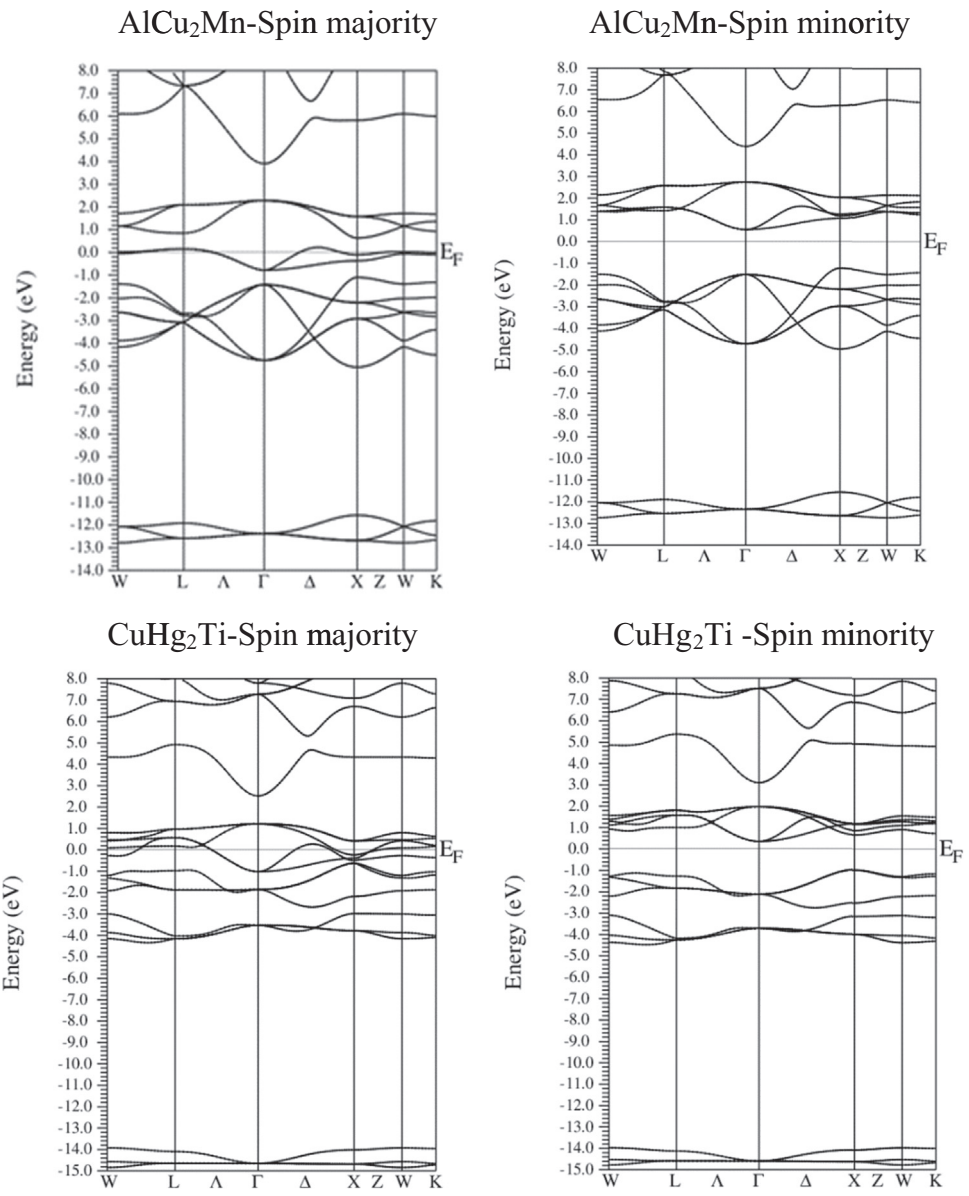

Fig. 2. The band structures of $KTiO_2$ compound for $AlCu_2Mn$ and $CuHg_2Ti$-type structures at the equilibrium lattice parameter. The solid line at zero eV indicates the Fermi energy (E_F).

level is located within a band gap. Therefore, this compound has a metallic characteristic for majority spin state, while it is a semiconductor in minority spin state, indicating HM characteristic of $KTiO_2$ in both structures. According to Figs. 3 and 4, KVO_2 in $CuHg_2Ti$-type and $KCrO_2$ in $AlCu_2Mn$-type structure are half-metal. KVO_2 in $AlCu_2Mn$-type structure is a special case since there is a relatively large energy gap in both spin directions, and the gaps are located at the same energy region resulting in a ferromagnetic semiconducting behavior. For $KCrO_2$ in $CuHg_2Ti$-type structure, the Fermi level crosses energy bands in both majority and minority spin states and there is a considerable difference between majority and minority states around the Fermi level. Therefore, this compound is a conventional ferromagnet. The band structure calculations (diagrams is not shown here) also indicate that $KCrC_2$, $KCrN_2$, KVC_2, and KVN_2 in both structures are conventional ferromagnets. Furthermore, $KTiC_2$ and $KTiN_2$ in both structures are nonmagnetic metals because the majority and minority spin states are completely similar and exhibit a metallic behavior.

In order to determine the characteristic of different bands in band structures, the band structure of $KTiO_2$ in both structures was investigated as a representative of all compounds. According to Fig. 2, in the $AlCu_2Mn$-type structure, the three bands between −13 and −12 eV and the six bands between −5 and −1 eV in both spin states are mainly relative to K p and O p states, respectively. In majority spin state, the two bands crossing the Fermi level is relative to Ti e_g states and the three bands between 1 and 2 eV belong to Ti t_{2g} states. In minority spin state, five Ti e_g and t_{2g} states are located between 0 and 3 eV above the Fermi level. In fact, the exchange splitting effect makes Ti e_g states move to higher energies in minority spin state, while this effect pushes them toward below the Fermi level in majority spin state. In $CuHg_2Ti$-type structure, the six O p bands are divided into two partitions between −5 and −1 eV and K p states are located between −15 and −14 eV. In majority spin state, the five Ti e_g and t_{2g} states joined together and cut the Fermi level, while in minority spin state, they are pushed above the Fermi level due to the exchange splitting effect.

Furthermore, the minority and HM (spin-flip) band gaps are

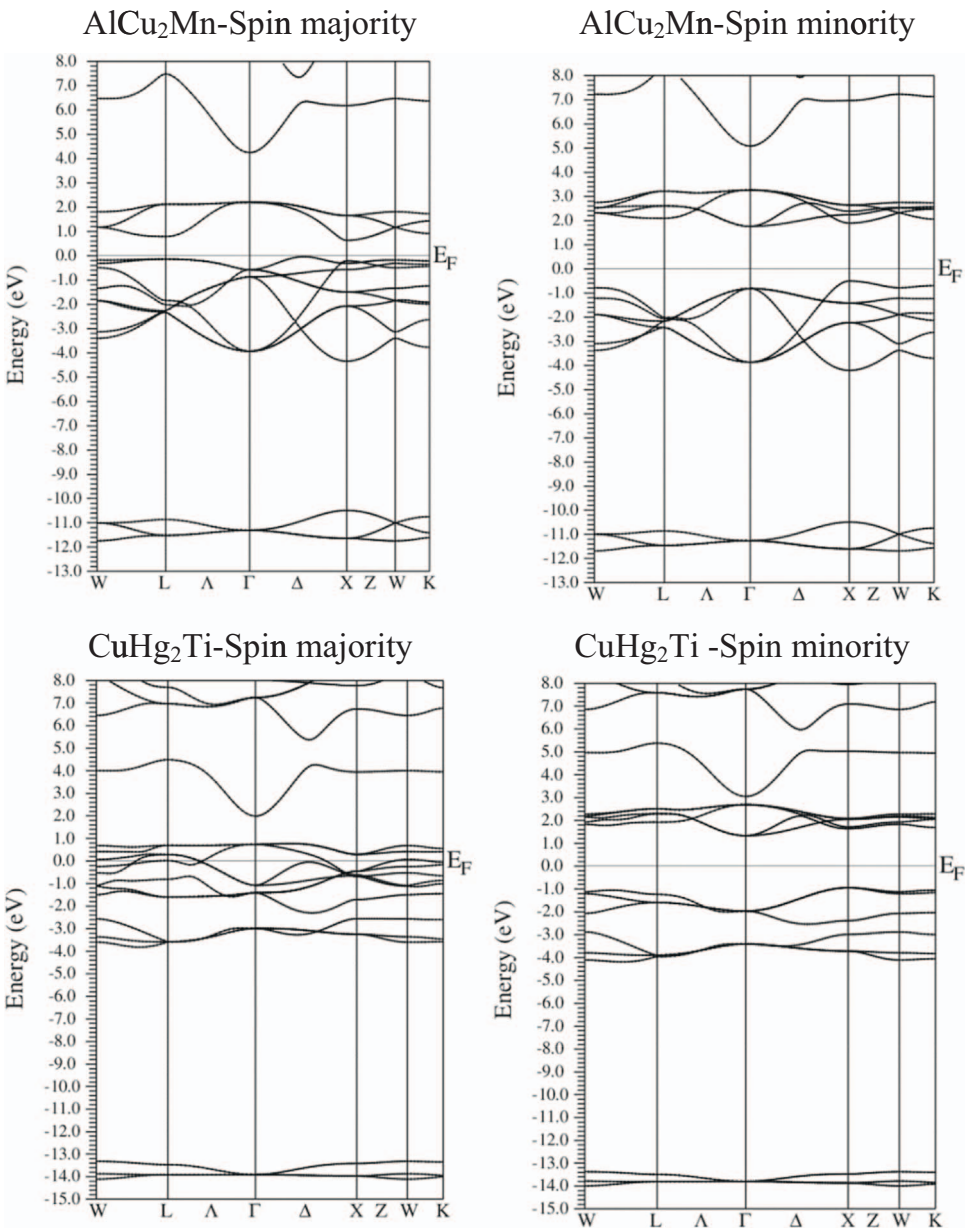

Fig. 3. The band structures of KVO_2 compound for $AlCu_2Mn$ and $CuHg_2Ti$-type structures at the equilibrium lattice parameter. The solid line at zero eV indicates the Fermi energy (E_F).

calculated and presented in Table 2. The minority band gap (E_g) is the difference between the energies of the highest occupied and the lowest unoccupied bands in the minority spin state. The HM band gap (E_{HM}), is defined as the minimum between the lowest energy of minority spin conduction bands with respect to the Fermi level and the absolute value of the highest energy of the minority spin valence bands. Values of E_g and E_{HM} for HM compounds are listed in Table 2. Among these compounds, $KCrO_2$ alloy has the highest E_g and E_{HM}. In Table 2, the values of E_{HM} are compared with those of Heusler alloys including or excluding transition metals. As can be seen, all three compounds have relatively wider band gaps in comparison with Heusler alloys containing transition metals. Furthermore, values of E_{HM} are approximately the same or higher than Heusler alloys excluding transition metals. This shows that HM character has been strengthened in the combined KYX_2 (Y=Ti, V, and Cr; X=C, N, and O) compounds.

It is important to find the origin of half-metallicty in the new half-metallic KYX_2 alloys. Therefore, total and partial density of states (DOSs) for $AlCu_2Mn$ and $CuHg_2Ti$-type structures of $KTiO_2$ as representative of all alloys were calculated and presented in Fig. 5. Accordingly, HM characteristic in both structures are confirmed because the majority spin states cut the Fermi level and the minority spin states are located within a band gap. In these compounds, two factors are effective in the formation of minority band gap. Firstly, this can be resulted from the bonding-antibonding splitting due to hybridization between the transition metal Ti *d* states and the O *p* states (between −5 and 3 eV in both structures). Secondly, the exchange splitting between majority and minority spin states around the Fermi level pushes the spin minority states above the Fermi level and causes majority spin states move below the Fermi level. In fact, this effect makes the Fermi level cross the electronic states in majority spin state and falls within a band gap in minority spin state. According to Fig. 5, the origin of half-metallicity in $CuHg_2Ti$-type structure is completely similar to $AlCu_2Mn$-type structure.

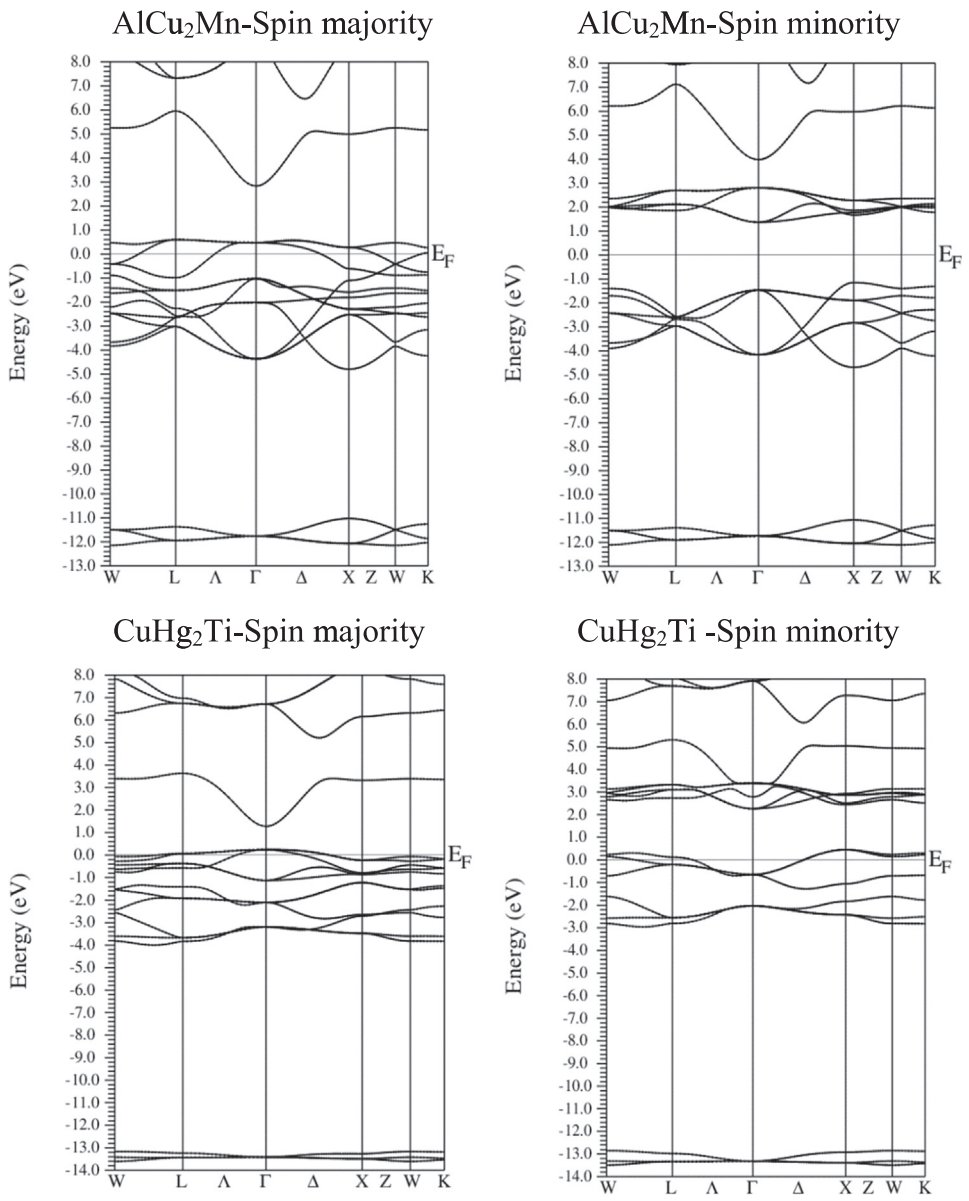

Fig. 4. The band structures of $KCrO_2$ compound for $AlCu_2Mn$ and $CuHg_2Ti$-type structures at the equilibrium lattice parameter. The solid line at zero eV indicates the Fermi energy (E_F).

3.3. The HM region

In order to examine the sensitivity of half-metallicity within uniform strain, the minority band gaps as a function of lattice constants are calculated for the four HM compounds (Fig. 6). It is found that HM character is kept between lattice constant values of 5.37–7.62 Å and 5.22–7.67 Å for $KTiO_2$ and $KCrO_2$ in the $AlCu_2Mn$-type structure and 5.60–6.91 Å and 5.29–6.99 Å for $KTiO_2$ and KVO_2 in $CuHg_2Ti$-type structure, respectively. The HM region for $KTiO_2$ and $KCrO_2$ in AlCu2Mn-type structure is considerably wider than that for $KTiO_2$ and KVO_2 in $CuHg_2Ti$-type structure. Furthermore, the regions of half-metallictiy in these compounds are considerably wider than those of Heusler compounds including transition metals [42–45]. With an overall view to Fig. 6, it is observed that there is a similar trend in all diagrams. With decreasing the lattice constant, the minority conduction band edge initially moves toward higher energies and subsequently shifts smoothly toward the Fermi level until the half-metallicity disappears. On the other hand, with increasing lattice parameter, the minority valence band edge changes smoothly and suddenly shifts toward the Fermi level and half-metallicty destroys.

3.4. Magnetic properties

HM materials usually have an integer total magnetic moment (M_{tot}) which is a requisite for these materials. Total and partial magnetic moments of KYX_2 (Y=Ti, V, and Cr; X=C, N, and O) compounds in $AlCu_2Mn$-type and $CuHg_2Ti$-type structures are listed in Table 3. Accordingly, the magnetic moments of $KTiC_2$ and $KTiN_2$ compounds in both structures are zero confirming NM characteristic of these compounds. M_{tot} for $KTiO_2$ and $KCrO_2$ in $AlCu_2Mn$-type structure and $KTiO_2$ and KVO_2 in $CuHg_2Ti$- type structure is an integer value which confirms HM character of these compounds. According to Fig. 2, for $KTiO_2$, the six minority spin p bands are completely filled with six electrons, while the majority spin p bands are filled with seven electrons which makes the M_{tot} equal to 1 μ_B. For $KCrO_2$ and KVO_2, the majority spin p bands filled with 9 and 8 electrons are responsible

Table 2
The calculated minority spin (E_g) and half-metallic (E_{HM}) band gaps of four HM compounds at equilibrium lattice constant. The values of E_{HM} are compared with those of Heusler alloys including or excluding transition metals.

Compound	*Structure*	E_g (eV)	E_{HM} (eV)
$KTiO_2$	$AlCu_2Mn$	1.77	0.54
$KTiO_2$	$CuHg_2Ti$	1.30	0.34
KVO_2	$CuHg_2Ti$	2.25	0.94
$KCrO_2$	$AlCu_2Mn$	2.50	1.16
[a]Co_2ScSb	$AlCu_2Mn$	0.38	0.24
[b]Mn_2CuSb	$CuHg_2Ti$	0.46	–
[c]Ti_2CoAl	$CuHg_2Ti$	0.49	0.17
[d]Ti_2CoGa	$CuHg_2Ti$	0.5	0.27
[e]$RbSrN_2$	$AlCu_2Mn$	5.3	0.73
	$CuHg_2Ti$	2.7	0.25
[e]$RbSrO_2$	$AlCu_2Mn$	4.7	0.46
	$CuHg_2Ti$	3.4	0.56
[f]$CsBaC_2$	$AlCu_2Mn$	1.67	0.18
[f]$CsBaN_2$	$AlCu_2Mn$	2.34	0.86
	$CuHg_2Ti$	2.29	0.72
[f]$CsBaO_2$	$AlCu_2Mn$	3.53	0.38
	$CuHg_2Ti$	2.76	0.61

[a] [42].
[b] [43].
[c] [44].
[d] [45].
[e] [37].
[f] [38].

for the magnetic moments of $3\mu_B$ and $2\mu_B$, respectively.

M_{tot} of HM materials, mainly obey the Slater-Pauling equation which relates M_{tot} to the total valence electrons (Z_{tot}) in the unit cell. The six p bands of O anion are occupied with six electrons. Thus, the number of occupied majority (spin-up) states ($N\uparrow$) is calculated as:

$$N\uparrow = Z_{tot} - N\downarrow = Z_{tot} - 6 \quad (1)$$

where $N\downarrow$ is the number of occupied minority (spin-down) states. Therefore, M_{tot} is calculated as:

$$M_{tot} = (N\uparrow - N\downarrow)\mu_B = (Z_{tot} - 2N\downarrow)\mu_B = (Z_{tot} - 12)\mu_B \quad (2)$$

The $KTiO_2$, KVO_2, and $KCrO_2$ compounds have respectively 13, 14, and 15 valence electrons and the M_{tot} are calculated equal to $1\mu_B$, $2\mu_B$, and $3\mu_B$ which are in a good agreement with the results of Table 3. Therefore Eq. (2) is a suitable Slater-Pauling equation for KYO_2 (Y=Ti, V, and Cr) compounds.

The M_{tot} of KYX_2 compounds consist from the four contributions: K atom, Y (Ti, V, and Cr) atom, X (C, N, and O) atom, and the interstitial region. According to Table 3, the main contribution to M_{tot} belongs to Y (Ti, V, and Cr) atoms. In all compounds, the magnetic moments of X and Y atoms are respectively negative and positive and the contribution of magnetic moments of K atom is negligible which show that atoms in KYX_2 compounds are in ferrimagnetic arrangement. Furthermore, magnetic moments in interstitial region are relatively considerable. The d states of Y(=Ti, V, and Cr) atom mainly exist inside the muffin-tin spheres, therefore hybridization between p states of X (=C, N, and O) atom with the Y d states makes the magnetic moments in interstitial region slightly increase.

Finally, the total and partial magnetic moments for $KTiO_2$ compound in the $AlCu_2Mn$-type and $CuHg_2Ti$-type structures as function of the lattice constant were shown in Fig. 7. It is clear that in both structures, M_{tot} is an integer value of $1\mu_B$ in a wide region of lattice parameter which shows that a moderate change in the lattice constant does not significantly affect HM characteristic. However, the partial spin moments of K, Ti, and O are quite sensitive to lattice distortion. As can be seen, the absolute values of O and Ti moments increase with increasing lattice constant. With expanding the lattice constant, the hybridization between O p and Ti d states decrease and spin moments of both atoms enhance. Similar behavior has also been observed in Heulser alloys [46]. The contribution of magnetic moment of K atom is negligible and expansion or contraction of lattice does not affect the magnetic moment of K atom.

4. Conclusion

The first principles calculations were performed to study the electronic structure and magnetic properties of new KYX_2 (Y=Ti, V, and Cr; X=C, N, and O) compounds in $AlCu_2Mn$-type and $CuHg_2Ti$-type structures. Calculations showed that $KTiO_2$ in both structures, $KCrO_2$ in $AlCu_2Mn$-type structure, and KVO_2 in $CuHg_2Ti$-type structure were HM ferromagnets, KVO_2 in $AlCu_2Mn$-type structure was a ferromagnetic semiconductor, and other compounds were conventional ferromagnets except $KTiC_2$ and $KTiN_2$ which were NM metals. Half-metallicty mainly originated from the hybridization between O p and Y(=Ti, V, and Cr) d states and splitting exchange effect. The values of M_{tot} for $KTiO_2$, KVO_2, and $KCrO_2$ were respectively 1, 2, and $3\mu_B$ which obeyed the Slater-Pauling rule (M_{tot}=Z_{tot}−12). Half-metallicity was preserved in the ranges of 5.37–7.62 Å and 5.22–7.67 Å for $KTiO_2$ and $KCrO_2$ in $AlCu_2Mn$-type structure and 5.60–6.91 Å and 5.29–6.99 Å for $KTiO_2$ and KVO_2 in $CuHg_2Ti$-type structure, respectively. The wider range of half-metallicity in KYO_2 (Y=Ti, V, and Cr) compounds with respect to Heusler alloys including transition metals introduces them as robust half-metals, which are interesting and attractive candidates for spintronic applications.

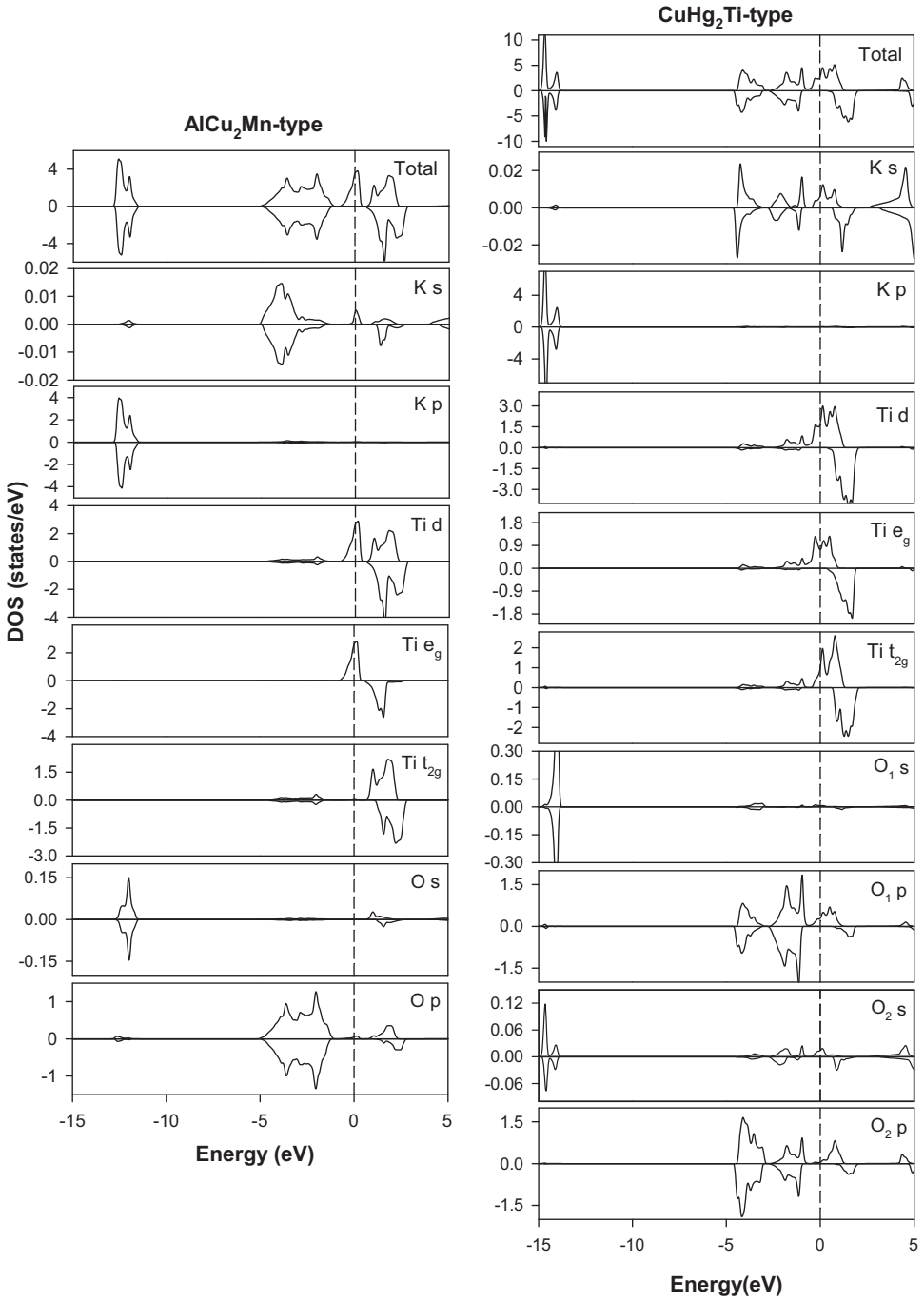

Fig. 5. The total and partial DOSs for the $KTiO_2$ compound for $AlCu_2Mn$ and $CuHg_2Ti$-type structures. Positive values of DOS are chosen as majority spin electrons and negative values as minority ones. The zero energy value corresponds to the Fermi level.

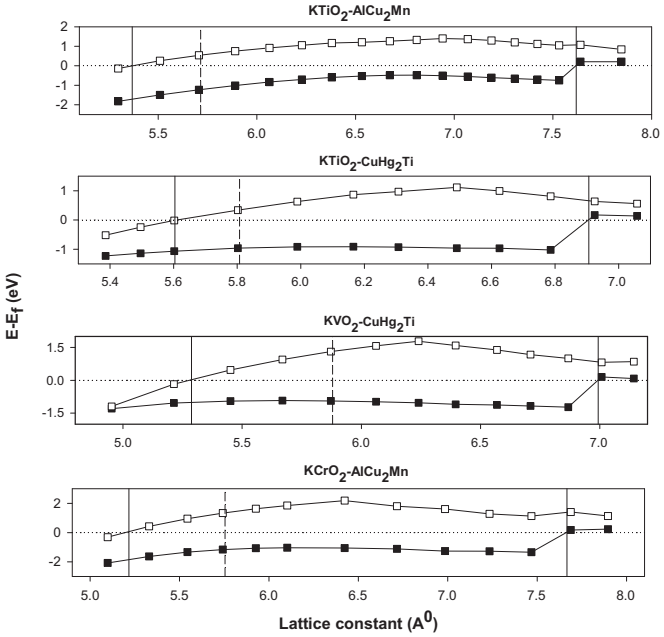

Fig. 6. The minority band gap of $KTiO_2$ in the $AlCu_2Mn$-type and $CuHg_2Ti$-type structures, $KCrO_2$ in the $AlCu_2Mn$-type, KVO_2 in $CuHg_2Ti$-type structure as a function of the lattice constant. The black and white squares show the valence band maximum (VBM) and conduction band minimum (CBM), respectively. The vertical dashed line indicates the equilibrium lattice constant and vertical solid lines show the range of half-metallicity. The horizontal dotted line at zero eV shows the Fermi energy.

Table 3
The total and atomic magnetic moments of KYX_2(Y=Ti, V, and Cr; X=C, N, and O) compounds in $AlCu_2Mn$-type and $CuHg_2Ti$-type structures. $M_{tot}(\mu_B)$: total magnetic moment; $M_K(\mu_B)$: K magnetic moment; $M_Y(\mu_B)$: Y magnetic moment; $M_X(\mu_B)$: X magnetic moment; and $M_{Int}(\mu_B)$: magnetic moment in the interstitial region.

Compound	*Structure*	M_{tot}	M_K	M_Y	M_{X1}	M_{X2}	M_{Int}
$KTiC_2$	$AlCu_2Mn$	0	0	0	0	0	0
	$CuHg_2Ti$	0	0	0	0	0	0
$KTiN_2$	$AlCu_2Mn$	0	0	0	0	0	0
	$CuHg_2Ti$	0	0	0	0	0	0
$KTiO_2$	$AlCu_2Mn$	1	0.02	0.86	−0.07	–	0.27
	$CuHg_2Ti$	1	0.03	1.12	−0.30	−0.23	0.37
KVC_2	$AlCu_2Mn$	1.94	0.02	1.60	−0.03	–	0.39
	$CuHg_2Ti$	2.77	0.05	2.24	0.03	−0.16	0.62
KVN_2	$AlCu_2Mn$	1.10	0	1.44	−0.56	–	0.19
	$CuHg_2Ti$	0.78	0.02	1.87	−0.85	−0.55	0.28
KVO_2	$AlCu_2Mn$	2	0.03	1.81	−0.17	–	0.41
	$CuHg_2Ti$	2	0.05	2.44	−0.57	−0.53	0.62
$KCrC_2$	$AlCu_2Mn$	2.85	0	2.63	−0.19	–	0.41
	$CuHg_2Ti$	3.14	0.05	3.05	−0.13	−0.28	0.44
$KCrN_2$	$AlCu_2Mn$	1.10	0.02	1.90	−1.02	—	0.24
	$CuHg_2Ti$	3.17	0.04	3.47	−0.28	−0.64	0.58
$KCrO_2$	$AlCu_2Mn$	3	0.02	3.13	−0.52	–	0.49
	$CuHg_2Ti$	5.95	0.04	3.59	1.2	0.43	0.69

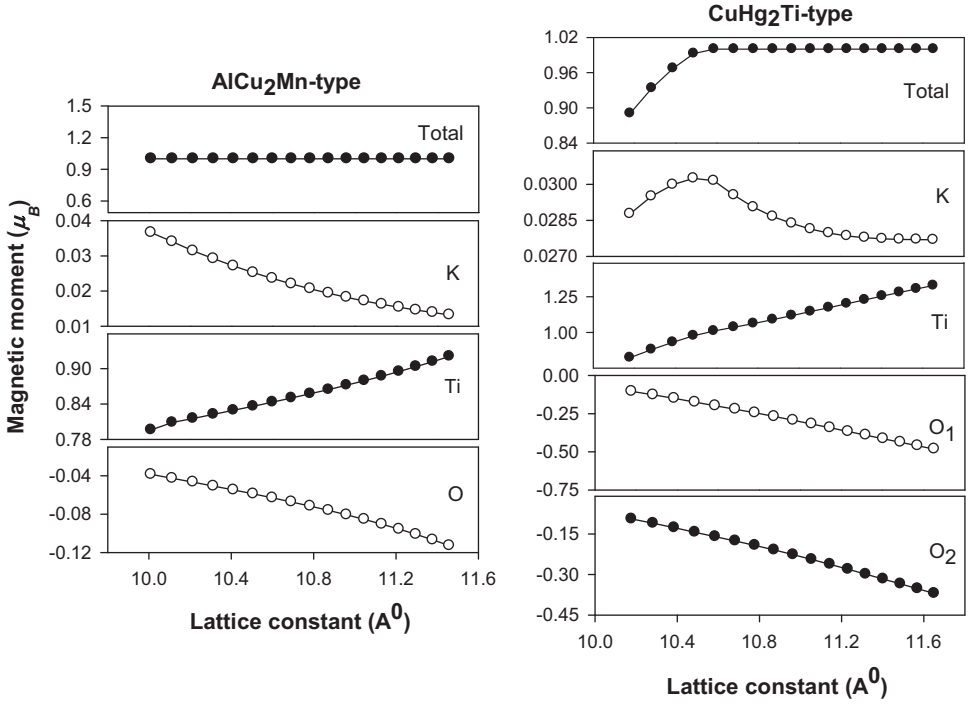

Fig. 7. Total and atomic magnetic moments as functions of the lattice constant for the $KTiO_2$ compound for $AlCu_2Mn$ and $CuHg_2Ti$-type structures.

References

[1] R.A. de Groot, F.M. Mueller, P.G. van Engen, K.H.J. Buschow, Phys. Rev. Lett. 50 (1983) 2024.
[2] M. Katsnelson, V.Y. Irkhin, L. Chioncel, A. Lichtenstein, R. De Groot, Rev. Mod. Phys. 80 (2008) 315.
[3] E. Şaşıoğlu, L.M. Sandratskii, P. Bruno, I. Galanakis, Phys. Rev. B 72 (2005) 184415.
[4] I. Galanakis, P.H. Dederichs, N. Papanikolaou, Phys. Rev. B 66 (2002) 174429.
[5] Y. Ji, G.J. Strijkers, F.Y. Yang, C.L. Chien, J.M. Byers, A. Anguelouch, G. Xiao, A. Gupta, Phys. Rev. Lett. 86 (2001) 5585.
[6] S. Soeya, J. Hayakawa, H. Takahashi, K. Ito, C. Yamamoto, A. Kida, H. Asano, M. Matsui, Appl. Phys. Lett. 80 (5) (2002) 823.
[7] T. Shishidou, A.J. Freeman, R. Asahi, Phys. Rev. B 64 (2001) 180401.
[8] Y. Tomioka, T. Okuda, Y. Okimoto, R. Kumai, K.I. Kobayashi, Y. Tokura, Phys. Rev. B 61 (2000) 422.
[9] J.H. Park, E. Vescovo, H.J. Kim, C. Kwon, R. Ramesh, T. Venkatesan, Nature 392 (1998) 794.
[10] L. Kronik, M. Jain, J.R. Chelikowsky, Phys. Rev. B 66 (2002) 041203.
[11] Y. Liu, B.-G. Liu, J. Phys. D40 (2007) 6791.
[12] H. Pan, Y.P. Feng, Q.Y. Wu, Z.G. Huang, J. Lin, Phys. Rev. B 77 (2008) 125211.
[13] K.L. Yao, G.Y. Gao, Z.L. Liu, L. Zhu, Y.L. Li, Physica B 366 (2005) 62.
[14] T. Graf, C. Felser, S.S.P. Parkin, Prog. Solid State Chem. 39 (2011) 14.
[15] P.J. Webster, K.R.A. Ziebeck, Alloys and Compounds of *d*-Elements with Main Group Elements, Springer, Berlin, 1988.
[16] K.R.A. Ziebeck, K.U. Neumann, Magnetic Properties of Metals, Springer, Berlin, 2001.
[17] C.M. Fang, G.A. de Wijs, R.A. de Groot, J. Appl. Phys. 91 (2002) 8340.
[18] S.A. Wolf, D.D. Awschalom, R.A. Buhrman, J.M. Daughton, S. Von Molnar, M.L. Roukes, A.Y. Chtchelkanova, D.M. Treger, Science 294 (2001) 1488.
[19] X.-Q. Chen, R. Podloucky, P. Rogl, J. Appl. Phys. 100 (2006) 113901.
[20] K. Özdoğan, I. Galanakis, E. Şaşıoğlu, B. Aktaş, Solid State Commun. 142 (2007) 492.
[21] V. Sharma, A.K. Solanki, A. Kashyap, J. Magn. Magn. Mater. 322 (2010) 2922.
[22] G.D. Liu, X.F. Dai, H.Y. Liu, J.L. Chen, Y.X. Li, Phys. Rev. B 77 (2008) 014424.
[23] S. Kervan, N. Kervan, Intermetallics 24 (2012) 56.
[24] S. Kervan, N. Kervan, Intermetallics 37 (2013) 88.
[25] I. Galanakis, K. Özdoğan, E. Şaşıoğlu, B. Aktaş, Phys. Rev. B 75 (2007) 172405.
[26] J. Li, Y.X. Li, G.X. Zhou, Y.B. Sun, C.Q. Sun, Appl. Phys. Lett. 94 (2009) 242502.
[27] N. Xing, Y. Gong, W. Zhang, J. Dong, H. Li, Comput. Mater. Sci. 45 (2009) 489.
[28] X.-P. Wei, J.-B. Deng, Ge-Y. Mao, S.-B. Chu, X.-R. Hu, Intermetallics 29 (2012) 86.
[29] Y.W. Son, M.L. Cohen, S.G. Louie, Nature 444 (2006) 347.
[30] O. Volnianska, P. Boguslawski, J. Phys. Condens. Matter 22 (2010) 073202.
[31] O. Volnianska, P. Boguslawski, Phys. Rev. B 83 (2011) 205205.
[32] K.L. Yao, J.L. Jiang, Z.L. Liu, G.Y. Gao, Phys. Lett. A 359 (2006) 326.
[33] G.Y. Gao, K.L. Yao, E. Sasioglu, L.M. Sandratskii, Z.L. Liu, J.L. Jiang, Phys. Rev. B 75 (2007) 174442.
[34] G.Y. Gao, K.L. Yao, Appl. Phys. Lett. 91 (2007) 082512.
[35] G.Y. Gao, K.L. Yao, N. Li, J. Phys. Condens. Matter 23 (2011) 075501.
[36] H. Rozale, A. Lakdja, A. Amar, A. Chahed, O. Benhelal, Comput. Mater. Sci. 69 (2013) 229.
[37] F. Bagverdi, F. Ahmadian, J. Supercond. Nov. Magn. 28 (2015) 2773.
[38] Z. Erfan, F. Ahmadian, J. Supercond. Nov. Magn. 28 (2015) 3301.
[39] P. Blaha, K. Schwarz, G.K.H. Madsen, D. Hvasnicka, J. Luitz, WIEN2k, an augmented plane wave local orbitals program for calculating crystal properties, Karlheinz Schwarz, Technische Universit Wien, Austria, 2001 (ISBN 3-9501031-1-2).
[40] J. Perdew, K. Burke, M. Ernzerhof, Phys. Rev. Lett. 77 (1996) 3865.
[41] F.D. Murnaghan, Proc. Natl. Acad. Sci. USA 30 (1947) 244.
[42] S. Kervan, N. Kervan, Intermetallics 19 (2011) 1642.
[43] X.-P. Wei, J.-B. Deng, S.-B. Chu, Ge-Y. Mao, L.-Bo Hu, M.-Kun Yang, X.-Ru Hu, Comput. Mater. Sci. 50 (2011) 1175.
[44] E. Bayar, N. Kervan, S. Kervan, J. Magn. Magn. Mater. 323 (2011) 2945.
[45] N. Kervan, S. Kervan, J. Magn. Magn. Mater. 324 (2012) 645.
[46] I. Galanakis, Ph Mavropoulos, P.H. Dederichs, J. Phys. D: Appl. Phys. 39 (2006) 765.